Consecutive Mechanism in the Diffusion of D_2O on a NaCl(100) Bilayer

Sarah-Charlotta Heidorn,[†] Cord Bertram,[‡] Pepa Cabrera-Sanfelix,[§,⊥] and Karina Morgenstern*[,‡]

[†]Leibniz Universität Hannover, Institut für Festkörperphysik, Abteilung für Atomare und Molekulare Strukturen (ATMOS), Appelstr. 2, D-30167 Hannover, Germany, [‡]Ruhr-Universität Bochum, Institut für Physikalische Chemie I, Universitätsstr. 150, D-44801 Bochum, Germany, [§]Donostia International Physics Center (DIPC), P. Manuel de Lardizabal 4, San Sebastian 20018, Spain, and [⊥]IKERBASQUE, Basque Foundation for Science, E-48011 Bilbao, Spain

ABSTRACT The motion of D_2O monomers is investigated on a NaCl(100) bilayer on Ag(111) between 42.3 and 52.3 K by scanning tunneling microscopy. The diffusion distance histogram reveals a squared diffusion lattice that agrees with the primitive unit cell of the (100) surface. From the Arrhenius dependence, we derive the diffusion energy, the pre-exponential factor, and the attempt frequency. The mechanism of the motion is identified by comparison of the experimental results to theoretical calculations. *Via* low temperature adsorption site determination in connection with density functional theory, we reveal an influence of the metallic support onto the intermediate state of the diffusive motion.

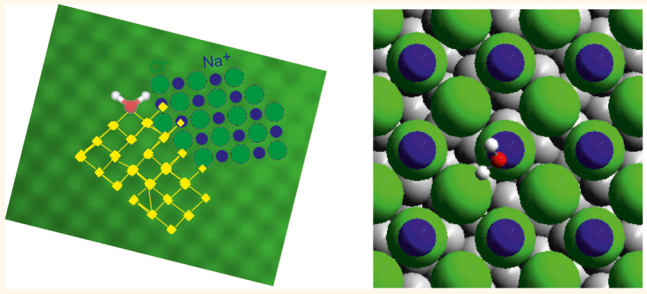

KEYWORDS: diffusion of adsorbates · water · salt · scanning tunneling microsopcy · density functional theory

Knowledge about the kinetics of water at surfaces is fundamental, because water is one of the most important substances in nature. Thereby, the water–salt system, in particular NaCl, is of specific interest because of its crucial role in areas as diverse as biophysics,[1,2] environmental physics,[3,4] and astrochemistry.[5,6] For example, the modeling of heterogeneous reactions in both the troposphere and on interstellar dust grains demands a detailed knowledge of the adsorption properties of water on salt. In addition, the diffusion of water on salt surfaces (NaCl) plays a fundamental role in the initial stages of solvation.[7] Though the interaction of water with NaCl is well understood from a macroscopic thermodynamic point of view, only few experiments have aimed at an understanding on the microscopic scale. Previous experimental work has concentrated mainly on a water coverage close to one complete layer, however, with controversial results.[8−10]

Diffusion of individual water molecules on NaCl has not been investigated experimentally yet, so that all current knowledge is based on DFT (density functional theory) calculations. Several groups agree that the preferred adsorption site of water on NaCl is close to the Na^+ ion with the hydrogen atoms pointing toward the Cl^- ion.[11−16] The reason for this adsorption site is that the Na−O bond is the stronger bond and the H−Cl bond gives only a minor contribution to the total adsorption energy. However, different orientations of the H atoms were predicted: the H atoms point either upward,[11] downward,[13−15] or are lying flat.[12] Only two groups have calculated the diffusive motion of water molecules on NaCl so far.[15,16] These calculations revealed that a simple translational motion without any changes in the molecule's orientation is energetically unfavorable because of the necessity to break all bonds.[15] Instead, the diffusion was predicted to consist of several consecutive steps.[15,16] Experimental evidence proving the consecutive steps in diffusion has not yet been obtained.

In this article, we present the first experimental study of water diffusion on NaCl(100) at the single molecule level. We investigate the diffusion of D_2O on bilayer high NaCl islands on Ag(111) between

* Address correspondence to karina.morgenstern@rub.de.

Received for review January 30, 2015 and accepted March 3, 2015.

Published online March 03, 2015
10.1021/acsnano.5b00691

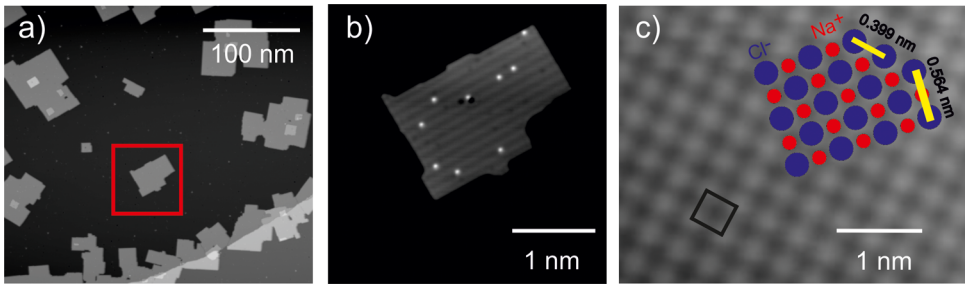

Figure 1. STM images of NaCl islands on Ag(111) with D_2O monomers: (a) Overview image (502 mV, 30 pA, 5 K). (b) Detailed image of the area marked in (a) with D_2O monomers visible as protrusions on the NaCl island (502 mV, 30 pA, 5 K). (c) Atomic resolution on NaCl (37 mV, 440 pA, 5 K). Primitive unit cell is indicated, schematic view of the NaCl(100) surface to scale with STM image. Yellow bars mark Cl−Cl distances of bulk crystal.

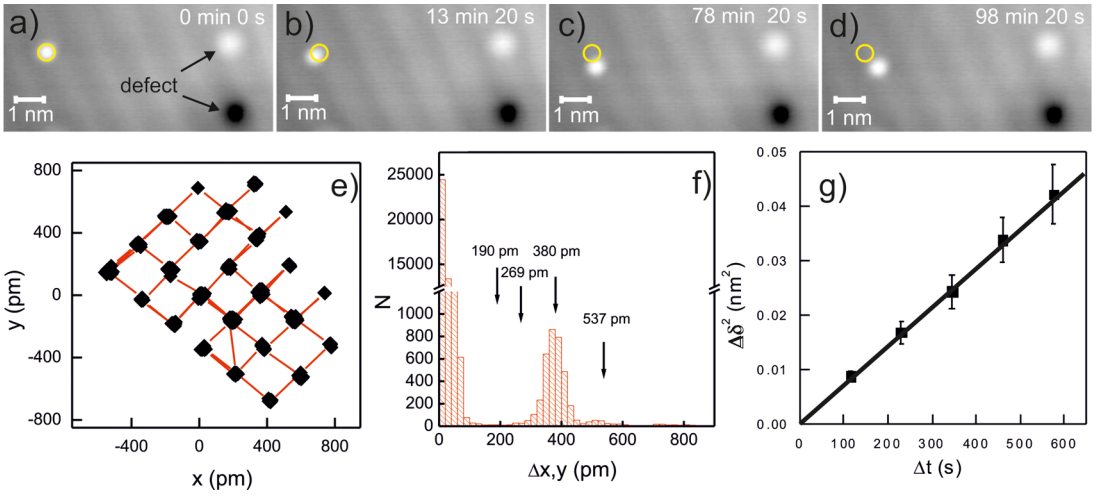

Figure 2. Diffusion of D_2O monomer at 46.8 K. (a−d) Snapshot of a STM movie taken at Δt = 100 s (image size 9 nm × 4 nm, 100 mV, 20 pA). Light circle marks position of molecule in first image. (e) Relative motion of the D_2O monomer marked in (a−d); note that positions from all 574 images of the movie are shown, not only those of the images a−d. (f) Diffusion length histogram. (g) Einstein plot with $\Delta\delta^2 = \Delta x^2$ or Δy^2. The linear fit yields $D = (7.2 \pm 0.1) \times 10^{-5}$ nm²/s.

42.3 and 52.3 K by scanning tunneling microscopy (STM). We ensure that the motion is random and determine the diffusion lattice as being squared, at a lattice constant of (380 ± 42) pm. This distance corresponds to the distance between Na^+ ions. From an Arrhenius plot, we derive a diffusion energy E_D of (149 ± 3) meV, a pre-exponential factor D_0 of 1.5 × $10^{11\pm0.2}$ nm²/s, and an attempt frequency ν_0 of 1.0 × $10^{12\pm0.2}$ Hz. Our results allow us to identify the rate limiting process among the predicted ones.

RESULTS AND DISCUSSION

Figure 1a shows an overview image of mostly bilayer high NaCl islands nucleated both on terraces and at step edges. D_2O diffusion is investigated on NaCl islands that are situated on terraces (*e.g.*, Figure 1b). The lattice parameters of the islands are determined from atomically resolved images as shown in Figure 1c. Note that in atomically resolved STM images of NaCl only the anions are imaged as protrusions.[17] The lattice constants of the primitive unit cell are (389 ± 6) pm and (383 ± 7) pm in the two perpendicular directions, at an angle of (90 ± 4)°. These values are in good agreement with those determined earlier.[21,22,26] D_2O molecules are imaged as protrusions (Figure 1b), at an apparent height of (51 ± 5) pm and a full width half-maximum of (0.86 ± 0.11) nm.

We now follow the motion of individual water molecules on NaCl by imaging the same spot of the surface repeatedly. A series of images is called a movie. Snapshots of such a STM movie are shown in Figure 2a−d, recorded at 46.8 K. In order to follow the motion of individual D_2O molecules in such movies, the center-of-mass of each molecule is determined *via* a two-dimensional Gaussian fit. Defects (right-hand side in Figure 2a−d) are used as markers to correct for a (tiny) residual thermal drift during the measurement. In order to minimize a possible influence of such defects onto the motion, we include only those D_2O molecules in the analysis that are at least four nanometers separated from such defects and other defects as island edges. The diffusion lattice is derived from the relative motion of the D_2O molecule (Figure 2e). It is quadratic. A statistical analysis reveals that the molecule diffuses with equal probability in all four directions of this lattice.

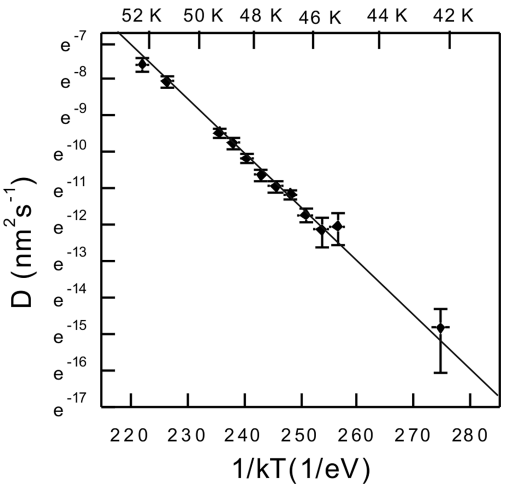

Figure 3. Arrhenius plot for D_2O diffusion on NaCl(100). The linear fit yields E_D = (149 ± 3) meV and D_0 = 1.5 × $10^{11\pm0.2}$ nm^2/s. The bar in *x*-direction marks the temperature range within a movie. The *y*-error bar is the statistical error.

The diffusion length histogram reveals three maxima (Figure 2f). The majority of the molecules are imaged at their original position, after 100 s at 46.8 K, leading to the main maximum at the origin. The maximum at (380 ± 42) pm corresponds to a motion of the molecule between neighboring ions (*cf.* Figure 1c). Finally, the maximum at (537 ± 34) pm corresponds to a motion to the next neighboring Na^+ ion. It thus represents molecules that diffused at least two lattice constants. Smaller diffusion distances between inequivalent ions ((1/2) · 380 pm = 190 pm) or between bridge sites ($(1/2)^{1/2}$) · 380 pm = 269 pm) are not observed (Figure 2f). We conclude that the molecules move between equivalent ions on the primitive unit cell of NaCl(100).

Diffusivity of D_2O on NaCl/Ag(111). Before analyzing the diffusivity, we have to ensure that the motion is a random motion. For this aim, we derive the mean-square distance of the diffusion for different time intervals and check for a linear dependence. As exemplified in Figure 2g this linear relationship is fulfilled.

We furthermore checked for a possible difference in diffusivity in the two scanning directions *x* and *y* as well as in the directions perpendicular and parallel to the Moiré pattern. In both cases, the diffusivities are identical within the error bars. Consequently, we may use the Einstein relation

$$D = \langle \Delta\delta^2 \rangle / (4\Delta t) \qquad (1)$$

with $\delta = x$ or *y* to determine the molecule's diffusivity.

Now we plot the direction-independent diffusivity *D* determined for different temperatures half-logarithmically *versus* 1/*kT* (Figure 3). As expected for an activated diffusion the data points follow a straight line. The Arrhenius law describes the temperature dependence of such an activated diffusion as[18]

$$D = D_0 \cdot e^{-E_D/(kT)} \qquad (2)$$

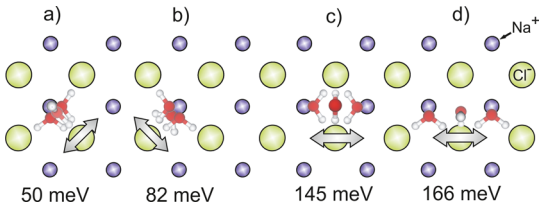

Figure 4. Top view of diffusion processes, adapted from the literature.[15,16] (a) OH-flip, (b) parallel rotation, (c) O-flip, (d) higher O-flip. For details, see text. Small blue circles correspond to Na^+, large green circles correspond to Cl^-, red circles correspond to O atoms, and white circles correspond to H atoms.

with E_D the activation or diffusion energy, *T* the temperature, *k* the Boltzmann constant, and D_0 the pre-exponential factor. In the case of two-dimensional single particle surface diffusion on a quadratic lattice, the pre-exponential factor D_0 is given by[18]

$$D_0 = l^2 \cdot \nu_0 \cdot e^{\Delta S_D/k} \qquad (3)$$

with *l* the diffusion length or lattice constant of the diffusion lattice and ν_0 the attempt frequency. ΔS_D is the entropy difference between ground state and transition state during the diffusive motion.

The Arrhenius plot covers 4 orders of magnitude from 10^{-3} to 10^{-7} $nm^2\ s^{-1}$ (Figure 3). This allows us to determine not only the diffusion energy E_D, but also the pre-exponential factor D_0 with high precision. The linear fit yields a diffusion energy of (149 ± 3) meV and a pre-exponential factor of 1.5 × $10^{11\pm0.2}$ nm^2/s. *Via* eq 3, we calculate $\nu_0 \cdot e^{\Delta S_D/k}$ = 1.0 × $10^{12\pm0.2}$ Hz. This value is within the expected range for surface diffusion of the attempt frequency $\nu_0 \approx 10^{12\cdots13}$ Hz.[18] It implies that only one degree of freedom, the frustrated translational vibration, is suppressed in the transition state. This result points to a simple hopping mechanism of the diffusion of D_2O on NaCl/Ag(111) similar to the one of atomic diffusion.

Interpretation of the Motion and Comparison to Theory. Having determined the diffusive lattice, the energy of motion, and the prefactor, we now compare these values to those calculated for different types of motion[15,16] in order to identify the most relevant ones. From the six calculated diffusion processes, two processes are not relevant. The so-called H-flip[15] has not been confirmed in a later study.[16] The parallel translation has, at 312 meV,[15] a much higher diffusion energy than determined here.

The remaining four processes can be classified into two categories. One category leads to a reorientation of the water molecule at the same Na^+ ion, not causing any large-scale mass transport itself (reorientation, in-cell motion, Figure 4a,b). During the OH-flip the molecule pivots by 180° around one of its OH-bonds (E_D = 50 meV, Figure 4a); during the parallel rotation the molecule rotates around a Na^+ ion (E_D = 82 meV, Figure 4b).

The other category leads to a motion from one Na^+ ion to a neighboring Na^+ ion (translation, out-of-cell motion, Figure 4c,d). During the O-flip the oxygen atom of the water rotates 180° around the axis formed by its two H-bonds, thus keeping the H-bonds pointing to the same Cl^- ions (E_D = 145 meV, Figure 4c); during the higher O-flip the molecule keeps only one of its H bonds to the Cl^- ion (E_D = 166 meV, Figure 4d).

The in-cell motions involve the breaking of one or both of the weaker H−Cl bonds and are therefore energetically preferred over the out-of-cell motion, during which the stronger Na−O is broken. However, at least one of the latter processes must be activated during the motion as in-cell motions alone cannot lead to a diffusive motion with large-scale mass transport.

The direction of motion is the same for both out-of-cell motions, but the distance differs, by which the center-of-mass of the molecule moves. Using the here determined lattice constant for bilayer NaCl of (386 ± 3) pm, the expected distance is (220 ± 3) pm for the O-flip, and (386 ± 3) pm for the higher O-flip.

There is some agreement to our experimental results, but none of the processes fits completely. While the higher O-flip has the diffusion length as observed in the diffusion histogram, the determined diffusion energy of (149 ± 3) meV is closest to the calculated diffusion energy of 145 meV of the O-flip.[16] The latter process should dominate because of its lower diffusion energy. Furthermore, the hopping rate of $\Gamma_{meas} = 3.1 \times 10^{12\pm0.2}$ Hz for 298 K as extrapolated from the Arrhenius plot agrees well with the one calculated for the O-flip in theory of $\Gamma_{theory} = 2.9 \times 10^{12}$ Hz at 298 K.[15]

Is it possible that we observe a larger distance than predicted theoretically? Noteworthy, a combination with one of the in-cell motions is mandatory for performing a large scale motion *via* the O-flip. Already at the lowest temperature, at which diffusion is observable on the time scale of the measurement (42.3 K), OH-flip and parallel rotation have rates of 1.1×10^7 Hz and 1.7×10^3 Hz, respectively. They thus happen frequently during the imaging time of a single molecule of approximately 2−3 s and are much too fast to be resolved.

This conclusion is supported by low temperature adsorption site determination. As the molecule cannot be imaged simultaneously with atomic resolution, we change the tunneling parameters on an image such that in the upper and lower part atomic resolution is achieved, but the molecules are imaged unperturbed in the middle of the image. The atomic lattice is then extended to this middle part and by this the relative position with respect to the sodium cation is determined. A multitude of adsorptions sites is obtained (Figure 5). All of them lie on a circle (140 ± 40) pm off the Na^+-on-top site. Within this circle there is no specific orientation indicative of a very shallow

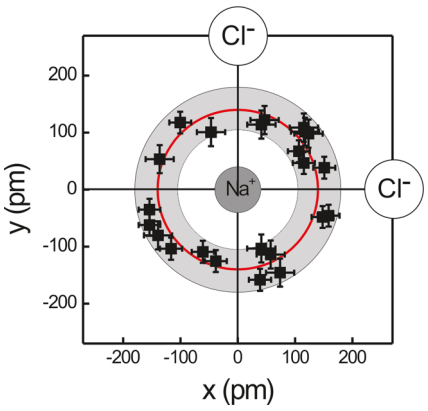

Figure 5. Adsorption sites measured at 5 K with respect to sodium ion; all molecules lie on a circle, at (140 ± 40) pm.

energy landscape for rotation of the molecule around the Na^+ ion.

The STM image at diffusion temperature thus represents the average over all possible rotational orientations. Consequently, we observe indeed a larger center-of-mass motion than predicted theoretically for the O-flip. We thus conclude that the O-flip in combination with the in-cell motions is responsible for the observed diffusion.

Though Figure 5 clarifies the diffusion data, it poses novel questions with respect to the adsorption site of water on the NaCl layer. Water monomers were calculated to be adsorbed slightly off the sodium site with the hydrogen atoms pointing toward the chlorine ions.[15,16] However, the potential energy surface is too corrugated to be consistent with the quasi-free rotation observed here. Different origins are possible. Tip effects can be safely excluded as the data is measured with different tips and positions within different quadrants of the plot are observed with the same tip. We thus concentrate on the differences between our measurement and the published calculations. These are 3-fold. First, we adsorb the water on a NaCl bilayer, while the calculation models bulk water. Second, the bilayer is adsorbed on a metal surface. Third, the calculated adsorption sites are calculated for 0.25 ML of water and not for single molecules. In fact, our present calculation find all differences to influence the water adsorption, the first one the total adsorption energy and the two latter once the relative adsorption energies between different water orientations.

We first compare the adsorption energies and adsorptions sites for 0.25 ML on NaCl layers of thicknesses ranging from 2 layers to 5 layers. The adsorption energies as shown in Table 1 are calculated with different functionals. The adsorption energy (E_{ads}) keeps constant with the number of layers for PBE, in which van-der-Waals corrections are not considered. However, for any other functional, which takes van-der-Waals interactions into account, E_{ads} increases with the number of layers as a consequence of the

long-range interactions. The increase of stability becomes constant, rising approximately 40 meV per added NaCl layer. The adsorption geometries, however, remain quite similar independent of slab thickness. Thus, the layer thickness is important, but it alone is not sufficient to explain the deviation in adsorption site.

This is different for single adsorbed molecules on a supported NaCl layer. Figure 6a,b shows several possible adsorption sites for a layer thickness of one and two layers, respectively. Table 2 lists adsorption energies annd the lateral displacements Δx and Δy of the oxygen atom of the water molecule from the Na ion underneath on a perfect NaCl lattice. Note that for one NaCl layer on Ag(111) not only the molecule is displaced during relaxation but the Na ion underneath the water is also slightly displaced from the perfect lattice position. For the one layer slab, the energy difference between the different sites is of the order of a few meV only (Table 2). These differences are so small that the first (i) and the third (iii) geometry can be considered to be degenerate in energy, and so one could consider that the water molecule may remain on this system either as symmetric planar molecule or as displaced and tilted molecules. Thus, the Ag(111) substrate underneath is affecting significantly the water adsorption. For the NaCl bilayer, the energy difference is of the order of 20 meV between the most stable configuration and the one following in stability, *i.e.*, the one in which the molecule is symmetrically placed and quasi planar with respect to the surface and the one in which the water molecule remains tilted and hydrogen bonded to only one Cl ion. Thus, two layers of NaCl screen the water interaction with the Ag substrate underneath better than only one NaCl layer. However, the differences between the adsorption energies are still small and confirm a rather shallow potential for the molecule around the sodium site, which can be overcome easily at the temperature of diffusion. An influence of the substrate onto water adsorption geometries on a NaCl layer was likewise calculated recently for Au(111), though in this study no deviation from the on-top site was found and the resulting geometry differed from ours.[19]

We conclude that though the electronic bulk properties of NaCl are already reached at bilayer thickness, the underlying metal still influences molecules adsorbed on it, here the adsorption site.

TABLE 1. Adsorption Energies in meV for 0.25 ML Water on Free Standing NaCl(100)

functional	2 layers	3 layers	4 layers	5 layers
PBE	388.9	384.5	387.5	387.5
optPBE-vdW	345.5	377.5	408.5	445.7
optPB86-vdW	347.2	385.5	423.9	460.3
optPB88-vdW	342.6	374.4	417.3	457.4

CONCLUSION

In conclusion, the diffusion of water on NaCl was investigated in real space. This represents the first

TABLE 2. Adsorption Energies and Geometrical Position of Structures Shown in Figure 6[a]

layer thickness	E_{ads} (meV)	Δx (pm)	Δy (pm)	structure
one layer	547.0	60.4	146.0	(i)
	542.5	43.6	181.3	(ii)
	551.4	9.9	97.5	(iii)
two layers	335.5	0.0	0.0	(i)
	314.4	0.0	0.0	(ii)
	343.5	3.5	52.4	(iii)
	363.3	0.0	74.4	(iv)

[a] Δx and Δy correspond to the displacement of the oxygen atom of the water molecule from the Na ion underneath on a perfect NaCl lattice.

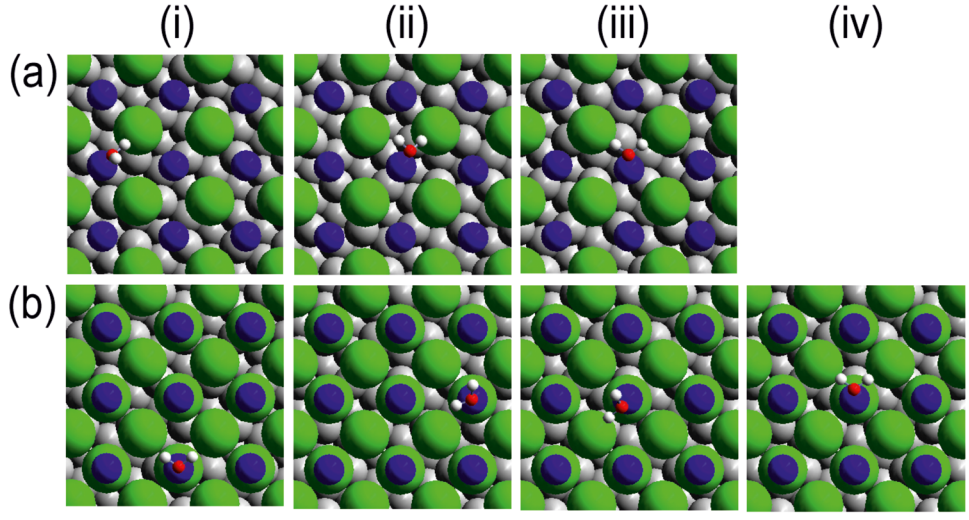

Figure 6. Adsorption geometries for single water molecule on (a) single NaCl layer on Ag(111) and (b) double NaCl layer on Ag(111). For energies and position values, see Table 2.

real-space diffusion study of a dipolar molecule on an ionic surface. The monomers diffuse on a squared diffusion lattice consistent with the primitive unit cell of NaCl(100). The motion consists of two consecutive processes, an out-of-cell motion that determines the diffusion energy of (149 ± 3) meV and a frequent reorientation around a shallow potential at (140 ± 40) pm distance from the sodium ion. The latter in-cell motion is altered by the metallic support as compared to diffusion on bulk NaCl. We suggest that layer thickness can be used to influence molecules, their diffusion, and consequently their reaction kinetics.

METHODS

STM measurements are performed with a low-temperature STM under ultrahigh vacuum (UHV) conditions (base pressure 2×10^{-10} mbar) at 5 K.[20] Ag(111) is cleaned by repeated cycles of Ne^+ sputtering and annealing. The sputtering is performed at a partial neon pressure of 3×10^{-5} mbar for 30 min at a sputtering current of 2 μA and an acceleration voltage of 1.3 keV. The sample is annealed for 30 min at 900 K. NaCl is evaporated from a Mo-crucible heated by electron bombardment with a rate of 0.02 monolayers/min. The sample is held during deposition at in between 292 and 305 K resulting in crystalline NaCl islands that grow mostly as (100) terminated bilayers.[21,22] The side length of the islands ranges from 28 to 35 nm.

D_2O of milli-Q quality is further cleaned in vacuum by freeze−thaw cycles. The chamber is flooded with D_2O prior to deposition in order to minimize the amount of H_2O resulting from the exchange reaction at the chamber walls. D_2O is deposited onto the sample positioned in the cold shields of the STM, at a deposition rate of 0.01 molecules/(nm^2s). During deposition, the sample surface temperature is held below 11 K, which is far below the diffusion temperature. D_2O adsorbs on NaCl nondissociatively.[23,24] A low coverage of 0.03 ML ensures that the D_2O is adsorbed as monomers.

STM images are taken in constant current mode. A brighter contrast implies a retraction of the tip from the sample. For a real-time tracking of the molecules, we scan the same spot of the surface repeatedly at regular time intervals between 62 and 180 s as established before.[25] Such movies are recorded at temperatures between 42.3 and 52.3 K. In total, 173 molecules were tracked yielding 81 000 data points.

Atomic resolution images were recorded at voltages between 16 and 100 mV. Larger images (overview images) are recorded at voltages up to 502 mV. The voltage used in the movies is 100 mV, and the tunneling current ranges from 20 to 30 pA. We checked for a possible influence of the scanning process on the diffusivity following a procedure developed earlier.[27] Most importantly, we compare diffusivities determined from two movies recorded at equivalent temperature and image acquisition time, but at different time intervals. This procedure changes the tip−sample interaction time, here by a factor of 6. The determined diffusivities are identical within the statistical error. The scanning process has thus no measurable influence on the diffusivity.

Density functional theory (DFT) has been applied to study the most favorable configuration for the adsorption of water at the submonolayer region (0.25 ML) on a thin slab of NaCl(100) and its dependence on the thickness of the NaCl slab, starting from two layers up to five. We use different approximations: PBE (not including van-der-Waals corrections)[28] and some of the new van-der-Waals functionals implemented in VASP: optPBE-vdW, optB86-vdW and optB88-vdW.[29,30] The lattice constant is always set to the correct value for each functional. We used a plane-wave cutoff of 400 eV and a K-point sampling $7 \times 7 \times 1$ Monkhorst-pack for the smallest cells, after checking the good convergence of relative values with $15 \times 15 \times 1$ Monkhorst-pack K-point sampling. The force criteria are ionic forces below 0.01 eV/atom and the electronic criterion is $dE = 10^{-5}$. In order to keep consistency, adsorption dependence on the NaCl thickness (from two to five layers) has been calculated by fixing all atoms except the top NaCl layer and the water molecule during relaxation.

To investigate the adsorption of a single water monomer on NaCl(001)/Ag(111), we relax one and two layers of NaCl(001)-(5×5) cell on three layers of Ag(111)-$(7 \times 4\sqrt{3})$, after having checked consistency by using five layers of Ag(111). The results presented in Table 2 correspond to optB88-vdW functional. Results were checked using PBE functional and although relative values changed depending on including van-der-Waals corrections or not, the general conclusions remained unaffected. The lattice constant mismatch is small, at an extension of the NaCl lattice parameter always below 2%. Because of the large number of atoms for all systems (221 and 271 atoms for one and two NaCl layers on 3 layers of Ag(111) respectively), the two bottom layers of Ag(111) are fixed during relaxation allowing the rest of atoms to relax, and the used number of K-points are set to Monkhorst−Pack $1 \times 1 \times 1$ for all calculations on these large supercell.

The calculation are performed with H_2O instead of D_2O to make calculations less expensive. Isotope effects do not compromise at all the comparison between experiments and theory as already checked in previous calculations of water diffusion on NaCl(100).[15] These calculations confirmed that water adsorption and energy barriers for diffusion are independent from using light or heavy water. Uniquely the diffusion coefficients, calculated following the Arrhenius's law, will change since they scale linearly with the molecule mass. This change is constant for all diffusion processes by comparing H_2O/D_2O, and therefore, the conclusions remained unaffected.

Conflict of Interest: The authors declare no competing financial interest.

Acknowledgment. We thank the German-Israeli Foundation for financial support. This work is supported by the Cluster of Excellence RESOLV (EXC 1069) funded by the Deutsche Forschungsgemeinschaft.

REFERENCES AND NOTES

1. Sung, S. S.; Jordan, P. C. Structures and Energetics of Nonovalent Ion−Water Microclusters. *J. Chem. Phys.* **1986**, *85*, 4045–4051.
2. Lin, S. N.; Jordan, C. Structures and Energetics of Monovalent Ion−Water Microclusters. II. Thermal Phenomena. *J. Chem. Phys.* **1988**, *89*, 7492–7501.
3. Russell, L. M.; Ming, Y. Deliquescence of Small Particles. *J. Chem. Phys.* **2002**, *116*, 311–324.
4. Hoose, C.; Möhler, O. Heterogeneous Ice Nucleation on Atmospheric Aerosols: A Review of Results from Laboratory Experiments. *Atmos. Chem. Phys.* **2012**, *12*, 9817–9828.
5. Hollenbach, D.; Salpeter, E. E. Surface Recombination of Hydrogen Molecules. *Astrophys. J.* **1971**, *163*, 155–164.
6. Finlayson-Pitts, B. J. The Tropospheric Chemistry of Sea Salt:? A Molecular-Level View of the Chemistry of NaCl and NaB. *Chem. Rev.* **2003**, *103*, 4801–4822.
7. Liu, L.-M.; Krack, M.; Michaelides, A. Interfacial Water: A First Principles Molecular Dynamics Study of a Nanoscale Water Film on Salt. *J. Chem. Phys.* **2009**, *130*, 2347021-12.
8. Fölsch, S.; Stock, A.; Henzler, M. Two-Dimensional Water Condensation on the NaCl(100) Surface. *Surf. Sci.* **1992**, *264*, 65–66.
9. Toennies, J. P.; Traeger, F.; Vogt, J.; Weiss, H. Low-Energy Electron Induced Restructuring of Water Monolayers on NaCl(100). *J. Chem. Phys.* **2004**, *120*, 11348–11350.
10. Cabrera-Sanfelix, P.; Darling, G. R.; Sanchez-Portal, D. On the Structure of the First Hydration Layer on NaCl(100): Role of Hydrogen Bonding. *J. Chem. Phys.* **2007**, *126*, 214707-1–214707-7.

11. Stöckelmann, E.; Hentschke, R. A Molecular-Dynamics Simulation Study of Water on NaCl(100) Using a Polarizable Water Model. *J. Chem. Phys.* **1999**, *110*, 12097–12106.
12. Meyer, H.; Entel, P.; Hafner, J. Physisorption of Water on Salt Surfaces. *Surf. Sci.* **2001**, *488*, 177–189.
13. Park, J. M.; Cho, J.-H.; Kim, K. S. Atomic Structure and Energetics of Adsorbed Water on the NaCl(001) Surface. *Phys. Rev. B: Condens. Matter Mater. Phys.* **2004**, *69*, 233403-1–233403-4.
14. Yang, Y.; Meng, S.; Wang, E. G. Water Adsorption on a NaCl (001) Surface: A density Functional Theory Study. *Phys. Rev. B: Condens. Matter Mater. Phys.* **2006**, *74*, 245409-1–245409-10.
15. Cabrera-Sanfelix, P.; Arnau, A.; Darling, G. R.; Sanchez-Portal, D. Water Adsorption and Diffusion on NaCl(100). *J. Phys. Chem. B* **2006**, *110*, 24559–24563.
16. Klimes, J.; Bowler, D. R.; Michaelides, A. A Critical Assessment of Theoretical Methods for Finding Reaction Pathways and Transition States of Surface Processes. *J. Phys.: Condens. Matter* **2010**, *22*, 074203−1–12.
17. Hebenstreit, W.; Redinger, J.; Horozova, Z.; Schmid, M.; Podloucky, R.; Varga, P. Atomic Resolution by STM or Ultrathin Films of Alkali Halides: Experiment and Local Density Calculations. *Surf. Sci. Lett.* **1999**, *424*, L321–L328.
18. Antczak, G., Ehrlich, G. *Surface Diffusion-Metals, Metal Atoms and clusters*. Cambridge University Press: New York, 2010.
19. Guo, J.; Meng, X.; Chen, J.; Peng, J.; Sheng, J.; Li, X.-Z.; Xu, L.; Shi, J.-R.; Wang, E.; Jiang, Y. Real-Space Imaging of Interfacial Water with Submolecular Resolution. *Nat. Mater.* **2014**, *13*, 184–188.
20. Mehlhorn, M.; Gawronski, H.; Nedelmann, L.; Grujic, A.; Morgenstern, K. An Instrument to Investigate Femtochemistry on Metal Surfaces in Real Space. *Rev. Sci. Instrum.* **2007**, *78*, 033905-1–033905-7.
21. Matthaei, F.; Heidorn, S.; Boom, K.; Bertram, C.; Safiei, A.; Henzl, J.; Morgenstern, K. Coulomb Attraction During the Carpet Growth Mode of NaCl. *J. Phys.: Condens. Matter* **2012**, *24*, 354006-1–354006-6.
22. Heidorn, S.; Bertram, C.; Koch, J.; Boom, K.; Matthaei, F.; Safiei, A.; Henzl, J.; Morgenstern, K. Influence of Substrate Surface-Induced Defects on the Interface State between NaCl(100) and Ag(111). *J. Phys. Chem. C* **2013**, *117*, 16095–16103.
23. Henderson, M. A. The Interaction of Water with Solid Surfaces: Fundamental Aspects Revisited. *Surf. Sci. Rep.* **2002**, *46*, 1–308.
24. Ewing, G. E. Ambient thin Film Water on Insulator Surfaces. *Chem. Rev.* **2006**, *106*, 1511–1522.
25. Morgenstern, K. Fast Scanning Tunnelling Microscopy as a Tool to Understand Changes on Metal Surfaces: From Nanostructures to Single Atoms. *Phys. Status Solidi B* **2005**, *242*, 773–796.
26. Heidorn, S.; Sabellek, A.; Morgenstern, K. Size Dependence of the Dispersion Relation for the Interface State between NaCl(100) and Ag(111). *Nano Lett.* **2014**, *14*, 13–17.
27. Morgenstern, K.; Rosenfeld, G.; Poelsema, B.; Comsa, G. STM-Imaging of Nanostructure Dynamics on Ag(111)-Experimental Challenges and Solutions. *Surf. Sci.* **1996**, *352−354*, 956–959.
28. Perdew, J. P.; Burke, K.; Ernzerhof, M. Generalized Gradient Approximation Made Simple. *Phys. Rev. Lett.* **1996**, *77*, 3865–3868.
29. Klimes, J.; Bowler, D. R.; Michealides, A. Van der Waals Density Functionals Applied to Solids. *Phys. Rev. B: Condens. Matter Mater. Phys.* **2011**, *83*, 195131-1–195131-13.
30. Klimes, J.; Bowler, D. R.; Michealides, A. Chemical Accuracy for the van der Waals Density Functional. *J. Phys. Condens. Mater.* **2012**, *22*, 022201-1–022201-5.